The Quiescent Counterpart of the Soft Gamma-Ray Repeater SGR 0526-66

doi: 10.1086/346110

The Astrophysical Journal, 585:948–954, 2003 March 10

THE QUIESCENT COUNTERPART OF THE SOFT GAMMA-RAY REPEATER SGR 0526−66

S. R. Kulkarni,[1] D. L. Kaplan,[1] H. L. Marshall,[2] D. A. Frail,[3] T. Murakami,[4] and D. Yonetoku[4]

Received 2002 September 21; accepted 2002 November 13

ABSTRACT

It is now commonly believed that soft gamma-ray repeaters (SGRs) and anomalous X-ray pulsars (AXPs) are magnetars—neutron stars powered by their magnetic fields. However, what differentiates these two seemingly dissimilar objects is, at present, unknown. We present *Chandra* observations of RX J052600.3−660433, the quiescent X-ray counterpart of SGR 0526−66, famous for the intense burst of 1979 March 5. The source is unresolved at the resolution of *Chandra*. Restricting observations to a period range around 8 s, the period noted in the afterglow of the burst of 1979 March 5, we find evidence for a similar periodicity in two epochs of data obtained 20 months apart. The secular period derivative based on these two observations is $6.6(5) \times 10^{-11}$ s s^{-1}, similar to the period derivatives of the magnetars. As is the case with other magnetars, the spectrum is best fitted by a combination of a blackbody and a power law. However, quite surprisingly, the photon index of the power-law component is $\Gamma \sim 3$—intermediate to those of AXPs and SGRs. This continuum of Γ led us to suggest that the underlying physical parameter that differentiates SGRs from AXPs is manifested in the power-law component. Two decades ago, SGR 0526−66 was a classical SGR, whereas now it behaves like an AXP. Thus, it is possible that the same object cycles between the SGR and AXP states. We speculate that the main difference between AXPs and SGRs is the geometry of the B fields, and this geometry is time dependent. Finally, given the steep spectrum of RX J052600.3−660433, the total radiated energy of RX J052600.3−660433 can be much higher than traditionally estimated. If this energy is supplied by the decay of the magnetic field, then the inferred B field of RX J052600.3−660433 is in excess of 10^{15} G, the traditional value for magnetars. Independent of this discussion, there could well be a class of neutron stars, 10^{14} G $\lesssim B \lesssim 10^{15}$ G, which are neither radio pulsars nor magnetars.

Subject headings: pulsars: individual (SGR 0526−66) — stars: neutron — X-rays: stars

1. INTRODUCTION

The soft gamma-ray repeater SGR 0526−66 played a key role in our understanding of high-energy transients. It was from this source that an intense burst was observed on 1979 March 5 (Mazets et al. 1979; Cline et al. 1980). The burst was followed by an "afterglow" emission with an apparent 8 s periodicity. The source of the burst was quickly localized to the supernova remnant N49 (also known as SNR 0525−66.1) in the Large Magellanic Cloud (Evans et al. 1980). Observations with *ROSAT* identified a quiescent and bright ($L_X \sim 10^{36}$ ergs s^{-1}) X-ray counterpart, RX J052600.3−660433 (Rothschild, Kulkarni, & Lingenfelter 1994).

The intense burst of 1979 March 5 and the luminous afterglow with 8 s periodicity provided the first and strongest evidence for superstrong magnetic field strengths, $B \sim 10^{15}$ G. Such strong fields are needed to both confine the radiating plasma as well as allow the radiation to escape (Duncan & Thompson 1992; Paczyński 1992). However, such highly magnetized neutron stars or "magnetars" were originally motivated by theoretical considerations—namely, strong convection would naturally lead to the growth of magnetic fields during the process of the collapse of the proto–neutron star core (Duncan & Thompson 1992; Thompson & Duncan 1993).

Separately, another group of neutron stars, the so-called anomalous X-ray pulsars (AXPs), were recognized as a new class of neutron stars (van Paradijs, Taam, & van den Heuvel 1995; Mereghetti & Stella 1995). The AXPs were noted for a narrow period distribution, between 6 and 20 s; luminous X-ray emission, $L_X \sim 10^{35}$ ergs s^{-1}; and apparent lack of a donor star. The sources were "anomalous" in that the source of the quiescent emission was neither rotational (from the known $\dot{P}$) nor accretion (apparent lack of companion). Various authors speculated and suggested that AXPs are also magnetars—specifically, that their X-ray emission arises from the decay of a magnetar-like field strength (Thompson & Duncan 1993).

The discovery of periodicity in SGRs (Kouveliotou et al. 1998) and the overlap of P and $\dot{P}$ between AXPs and SGRs continued to motivate a unified magnetar framework for both these objects. In particular, the magnetic field strength inferred from P and $\dot{P}$ (vacuum dipole framework) led to estimates of about 10^{14} G for both these objects, within a factor of a few of that estimated for AXPs and SGRs.

Toward the end of the 1990s, thanks to large-area radio pulsar searchers, astronomers became aware of a growing group of radio pulsars (Camilo et al. 2000) with similarly long periods and with inferred magnetic field strengths approaching 10^{14} G (hereafter HBPSRs). These pulsars possess no special attributes linking them to either the AXPs (no steady bright quiescent X-ray emission; Pivovaroff, Kaspi, & Camilo 2000) or the SGRs (no bursting history). Thus, periodicity alone does not appear to be a sufficient attribute for classification.

[1] Division of Physics, Mathematics and Astronomy, 105-24, California Institute of Technology, Pasadena, CA 91125; srk@astro.caltech.edu.

[2] Center for Space Research, Massachusetts Institute of Technology, Cambridge, MA 02139.

[3] National Radio Astronomy Observatory, P.O. Box O, Socorro, NM 87801.

[4] Department of Physics, Kanazawa University, Kadoma-cho, Kanazawa 920-1192, Japan.

Nonetheless, the recent discovery of bursts of radiation—similar to the minor bursts seen from SGRs—from two AXPs is strong empirical confirmation of a link between AXPs and SGRs (Gavriil, Kaspi, & Woods 2002; Kaspi & Gavriil 2002). However, we are still at a loss as to what specific physical parameter(s) differentiate(s) AXPs from SGRs.

One plausible notion is that AXPs and SGRs are linked temporally. Specifically, three of the six AXPs are associated with supernova remnants (SNRs), whereas only SGR 0526−66 has a plausible SNR association (Gaensler et al. 2001). Taken at face value, these data suggest that AXPs evolve into SGRs. However, this hypothesis has two problems. First, the rotational periods of SGRs are similar to those of AXPs, about 10 s. Second, inferred magnetic field strengths of SGRs are similar to (and perhaps even larger than) those of AXPs (Hurley 2000; Mereghetti 2001). Thus, there is no strong period or *B*-field evolution between the two groups.

In our opinion, the above two objections are sufficiently severe that we must continue searching for underlying physical parameter(s) that differentiate(s) between AXPs and SGRs. To this end, investigating the properties of the quiescent emission, which in practice means spectroscopic and rotational properties, appears promising. Here we report an investigation of the quiescent X-ray emission of SGR 0526−66, comparing and contrasting the quiescent emission with those of AXPs and other SGRs.

2. OBSERVATIONS AND ANALYSIS

We observed RX J052600.3−660433 thrice with the *Chandra X-Ray Observatory* (Weisskopf et al. 2000). Our goal was to search for periodicity and obtain a broadband spectrum of RX J052600.3−660433. To this end the first two observations were obtained with a high temporal resolution. Specifically, the back-side–illuminated ACIS-S3 charge-coupled device (CCD) was used in a 1/8 subarray mode with a frame read every 0.44104 s. The first observation (ObsId 747) began at 4.02 January 2000; the total on-source integration time was 37.2 ks. The second observation (ObsId 1957) used the same CCD setup and started on 31.94 August 2001; the total integration time was 46.5 ks. The last observation (ObsId 2515) was designed to image the entire SNR, and hence we used the entire S3 chip with a frame time of 3.2 s and an integration time of 6.8 ks.

All data sets were processed identically. First, we reprocessed the level 1 event data with the CIAO tool *acis_process_events* to account for updated gain maps and geometric calibration of the spacecraft.[5] We then produced a level 2 event file by copying only events with the correct grades.[6] With this file, we restricted the data to the energy range of 0.3–10 keV and filtered out times of high background count rates. Finally, we barycentered the data with the *axBary* tool using the position of RX J052600.3−660433 (§ 2.1).

2.1. *Image Analysis*

The subarray observations resulted in images with size 128×1024 pixels, whereas the full-frame observation resulted in a 1024×1024 pixel image (see Fig. 1). The source RX J052600.3−660433 is very well detected: in the first subarray observation a total of 9391 events were detected in a 3.5 pixel radius and energy range 0.3–10 keV, over the estimated integration time of 37,527 s, while in the second subarray observation we detected 11,148 counts over 49,019 s. In both cases, the background has not been subtracted. Background subtraction is tricky given the high level of background (we will revisit this topic later). We see that the count rate is noticeably different between the two visits.

TABLE 1
POSITION OF RX J052600.3−660433

ObsId	x (pixels)	y (pixels)	$\alpha - 05^{h}26^{m}$ (s)	$\delta + 66°04'$ (arcsec)
747	4160.596(8)	4135.884(8)	00.8791(6)	−36.180(4)
1957	4090.665(8)	4025.371(8)	00.9094(6)	−36.424(4)
2515	4091.27(3)	4025.06(3)	00.911(4)	−36.45(1)
Average	...	...	00.8948(4)	−36.307(3)

NOTE.—Positions are J2000. The values in parentheses above are 1 σ statistical uncertainties. There is an additional 1 σ position uncertainty of $\approx 0\farcs6$ in each coordinate due to aspect uncertainties.

Having detected the source, we fitted a one-dimensional Gaussian with $\sigma = 0\farcs33$ (corresponding to an FWHM = $0\farcs78$) in each axis to the events. The value of σ is comparable to that expected from a point source, and thus RX J052600.3−660433 is unresolved even at *Chandra*'s exquisite angular resolution.

After correcting for known aspect errors,[7] we fitted for the position of SGR 0526−66 using an iterative technique. First, we determined the mean x and y source positions (using σ-clipping with a 3 σ limit) of the events in a 3 pixel ($1\farcs5$) region around the nominal position of SGR 0526−66. We then used this new position to refine the center of the source region and iterated until the position converged (which occurred in 3–4 iterations depending on the data set). As can be seen from Table 1, the best fit position of RX J052600.3−660433 is right ascension $05^{h}26^{m}00\fs89$ and declination $-66°04'36\farcs3$ (equinox J2000); the photon (stochastic) error is negligible, and the error is dominated by $0\farcs6$ systematic error in each coordinate arising from uncertain aspect. This position can be compared with the *ROSAT* position of $05^{h}26^{m}00\fs3$ and $-66°04'33\farcs2$ with an uncertainty of 5″ (radius).

We inspected the image for evidence of a compact nonthermal nebula—a plerion—but found no evidence for one. However, strong diffuse emission from N49 is seen. Indeed, at a radius of 2″ we clearly detect thermal SNR emission replete with line features: Mg-K (1.25 keV), Si-K (1.74 keV), S-K (2.31 keV), and Ar-K (2.96 keV). Such a spectrum is typical of the emission expected from a middle-aged SNR (see also Table 2).

2.2. *Spectral Analysis*

For the spectral analysis, we used only the data from ObsId's 747 and 1957 because these were not affected by photon pileup. We extracted the counts from a region around the source position with a 2 pixel (1″) radius for

[5] See http://asc.harvard.edu/ciao/threads/geom_par.

[6] *ASCA* grades 0, 2, 3, 4, and 6.

[7] See http://asc.harvard.edu/cal/ASPECT/fix_offset/fix_offset.cgi.

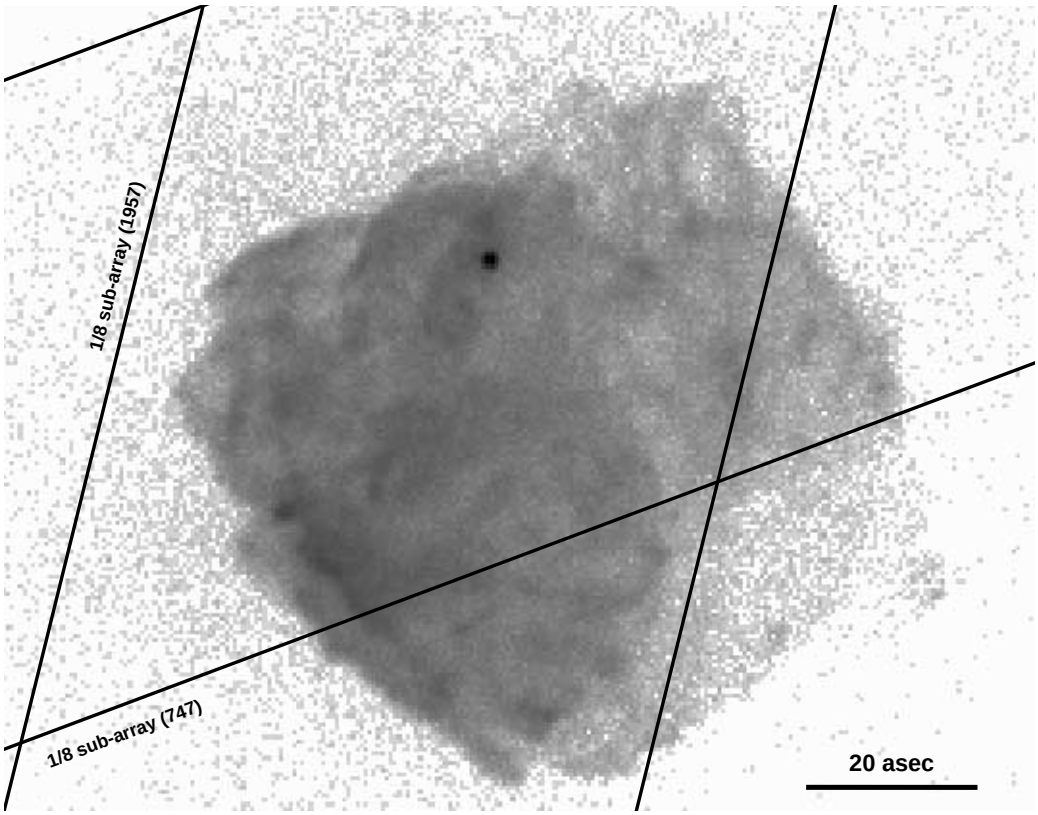

FIG. 1.—Image of SNR N49 obtained from the *Chandra* X-ray satellite. This image is a composite of all three observations binned to 1 pixel (0″.49) resolution. RX J052600.3−660433, the quiescent counterpart to SGR 0526−66, is the point source toward the top. The limited spatial regions covered by the subarrays (ObsID's 747 and 1957) are indicated by the parallel lines. A 20″ scale is shown, and the orientation follows the usual convention with north up and east to the left.

spectral analysis; for the background, we used an annulus with radius from 2 to 10 pixels (we use an aperture correction of 8% to account for the finite extraction aperture, determined using *mkpsf*). We then used the *psextract*[8] tool to bin the data and generate the necessary response files. The spectral data were binned to have 20 counts in each bin.

We fitted the data using three models: blackbody (BB), power law (PL), and power law plus blackbody (PL+BB), all modified by interstellar absorption (Balucinska-Church & McCammon 1992, assuming solar abundances). We required that both observations have the same interstellar absorption column density, $N_{\rm H}$. We tried two types of fits for each model: in type *a* the fit parameters were held to be the same over both observations, and in type *b* all parameters other than $N_{\rm H}$ were allowed to differ. The results of these four fits (two models and two types) are shown in Table 2.

The single-blackbody (BB) model produces unacceptable χ^2. The fit shows systematic deviations in the following bands: 0.5–0.8, 1.0–1.5, and 3.5–7.0 keV. Furthermore, the BB fit results in an inferred interstellar absorption column, $N_{\rm H}$, well below that obtained from analysis of the emission from the supernova remnant (SNR) N49 (see below). Thus, we decisively reject the BB model.

As can be seen from Table 2 and Figure 2, the PL and PL+BB models provide acceptable fits. To determine statistically which fit is the best, we used an *F*-test (see Bevington & Robinson 1992, p. 208). This test involves comparison of the difference in χ^2 values (between a given fit and the best-fit model) and the difference in degrees of freedom to the χ^2 value and degrees of freedom for the best-fit (PL+BB, type *b*) model. As seen in Table 2, complicated models are highly preferred over the simplest (PL type *a*) model: the type *b* PL+BB model is preferred at the 99.97% confidence level. This indicates that a blackbody component is preferred for the fit at the 90% confidence level and that while the power-law indices and blackbody temperatures are similar across the fits, there is a change in absolute flux, necessitating the type *b* model. This change is likely the result of the degradation of the ACIS detectors.[9]

Separately, we carried out a single-temperature MEKA-L model in *xspec* of the SNR emission close to RX J052600.3−660433 and obtained adequate fit kT of 0.21 keV and $N_{\rm H} = (6.4 \pm 0.1) \times 10^{21}$ cm^{-2}. (A more detailed analysis of the SNR spectrum is in progress.)

2.3. *Search for Periodicity*

For other SGRs, periodicity has been detected in the quiescent X-ray emission (Kouveliotou et al. 1998; Hurley et al. 1999). Marsden et al. (1996) searched unsuccessfully for periodicity from RX J052600.3−660433 in the *ROSAT*

[8] See http://asc.harvard.edu/ciao/threads/psextract.

[9] See http://asc.harvard.edu/cal/Acis/Cal_prods/qeDeg.

TABLE 2

SUMMARY OF SPECTRAL FITS TO RX J052600.3−660433

PARAMETER	MODEL TYPE			
	PL		PL + BB	
	Type *a*	Type *b*	Type *a*	Type *b*
N_H ($\times 10^{22}$ cm^{-2})	0.56(1)	0.56(1)	0.55(2)	0.54(2)
ObsId 747				
Γ	3.06(3)	3.06(4)	3.14(8)	3.1(1)
PL norm ($\times 10^{-3}$ s^{-1} cm^{-2} keV^{-1})	1.18(5)	1.22(5)	1.08(8)	1.13(8)
PL f_X[a] ($\times 10^{-12}$ ergs s^{-1} cm^{-2})	1.17	1.23	1.01	1.12
PL f_X^u ($\times 10^{-12}$ ergs s^{-1} cm^{-2})	3.56	3.68	3.26	3.39
kT^∞ (keV)	...	...	0.53(6)	0.6(1)
R_{BB}^∞ (km)[b]	...	...	$2.6(5)d_{50}$	$2(1)d_{50}$
BB f_X ($\times 10^{-12}$ ergs s^{-1} cm^{-2})	...	...	0.14	0.10
BB f_X^u ($\times 10^{-12}$ ergs s^{-1} cm^{-2})	...	...	0.22	0.13
f_X^u ($\times 10^{-12}$ ergs s^{-1} cm^{-2})	3.56	3.68	3.42	3.52
L_X ($\times 10^{36}$ ergs s^{-1})[b]	$1.01d_{50}^2$[c]	$1.04d_{50}^2$	$0.97d_{50}^2$[c]	$1.00d_{50}^2$
ObsId 1957				
Γ	3.06(3)[c]	3.06(4)	3.14(8)[c]	3.12(8)
PL norm ($\times 10^{-3}$ s^{-1} cm^{-2} keV^{-1})	1.18(5)[c]	1.14(4)	1.08(8)[c]	0.98(8)
PL f_X ($\times 10^{-12}$ ergs s^{-1} cm^{-2})	1.17[c]	1.14	1.01[c]	0.95
PL f_X^u ($\times 10^{-12}$ ergs s^{-1} cm^{-2})	3.57[c]	3.46	3.26[c]	2.95
kT^∞ (keV)	...	...	0.53(6)[c]	0.48(5)
R_{BB}^∞ (km)[b]	...	...	$2.6(5)d_{50}$[c]	$3(1)d_{50}$
BB f_X ($\times 10^{-12}$ ergs s^{-1} cm^{-2})	...	...	0.14[c]	0.16
BB f_X^u ($\times 10^{-12}$ ergs s^{-1} cm^{-2})	...	...	0.22[c]	0.28
f_X^u ($\times 10^{-12}$ ergs s^{-1} cm^{-2})	3.57[c]	3.46	3.42[c]	3.26
L_X ($\times 10^{36}$ ergs s^{-1})[b]	$1.01d_{50}^2$[c]	$0.98d_{50}^2$	$0.87d_{50}^2$[c]	$0.92d_{50}^2$
DOF	332	330	330	326
χ^2/DOF	1.06	1.03	1.03	1.00
$P(PL_a)$[d]	...	3×10^{-3}	3×10^{-3}	3×10^{-4}

NOTE.—All fluxes and luminosities are in the 0.5–10 keV range. Values in parentheses are 1 σ statistical uncertainties.

[a] The power-law (PL) normalization is at 1.0 keV.

[b] At a distance of $50d_{50}$ kpc.

[c] Fixed to be the same as the corresponding value for ObsId 747.

[d] Probability that the type *a* PL model is preferred over the specified model.

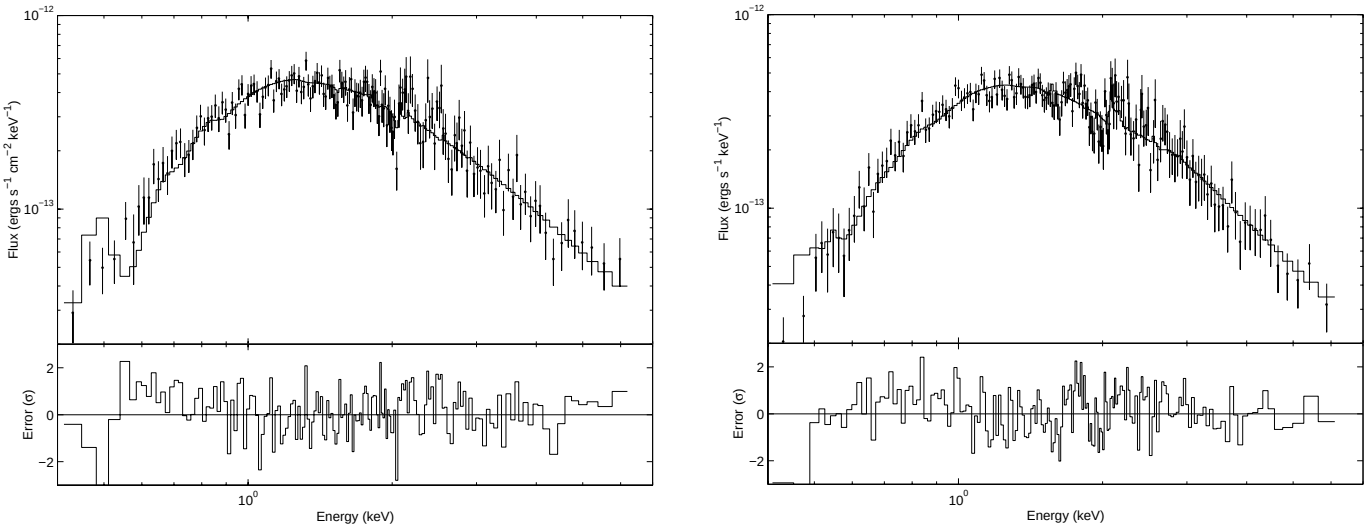

FIG. 2.—*Chandra* spectra of SGR 0526−66, from 0.4 to 6 keV. The data are shown as points, with the best-fit PL+BB (type *b*) models (see Table 2) shown as solid lines. The lower panels show the residuals, in units of σ. The data are ObsId 747 (*left*) and ObsId 1957 (*right*). The fits are in general quite good. The "features" near 1.75 and 2.5 keV are from improperly subtracted nebular emission (from Si and S, respectively), likely due to the spatial variations of thermal emission from SNR N49.

data, but their limit of 66% pulse fraction was not very stringent.

We used the well-known statistic Z_n^2 (de Jager, Raubenheimer, & Swanepoel 1989) to search for periodicity. After transforming the arrival times of the events in ObsID 747 to the barycenter of the solar system, we added a random number drawn uniformly from the range [0.0, 0.44104] s to remove any artifacts created by the readout process. We began searching with the Z_1^2 statistic around a range encompassing the previously noted period (7.9–8.1 s) but found no significant peak. Reinspecting the pulsations in the afterglow of 1979 March 5, we noted that the interpulse gets stronger toward the end of the afterglow of 1979 March 5 (Cline et al. 1980). A strong interpulse located 180° in phase from the main pulse will result in weakening the fundamental and the second harmonic. Motivated thusly, we searched with the Z_2^2 statistic, which incorporates power from the first harmonic in the periodogram, and found a peak of moderate significance at 8.0436(2) s (Fig. 3).

Using this detection as a starting point, we searched for related periodicities in the ObsID 1957 data. We find a peak of similar strength in the Z_2^2 periodogram at 8.0470(2) s (see Fig. 3). Here, though, while the strength of the peak is similar in the two observations, the significance is higher in the second because we can restrict the region searched in period space to those values allowed by the range of expected period derivatives ($0 \text{ s s}^{-1} \leq \dot{P} \leq 10^{-10} \text{ s s}^{-1}$, or 8.0436–8.0488 s; although we show the full 7.9–8.1 s in Fig. 3 for clarity). With this restricted range, the significance of the second periodicity increases to ~99.98%. The secular spin-down inferred from these two observations is $6.5(5) \times 10^{-11}$ s s^{-1}, in the range found for SGRs and AXPs (Hurley 2000; Mereghetti 2001).

As can be inferred from the marginal detection, the pulse fraction is quite low, $F \sim 10\%$, where $F = \text{mean}(\text{LC})/\min(\text{LC}) - 1$, where mean (LC) is the mean of the light curve and min(LC) is the minimum of the light curve.

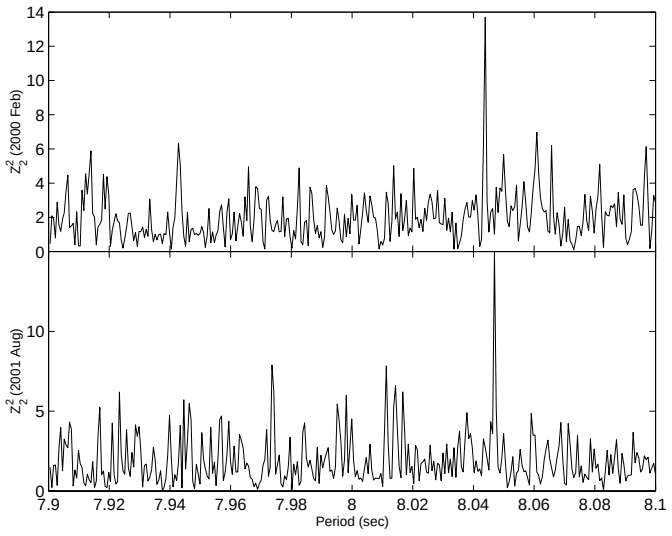

FIG. 3.—Z_2^2 periodograms of ObsID 747 (*top*) and ObsID 1957 (*bottom*) showing the most probable periodicities of 8.0436(2) and 8.0470(2) s, respectively. The nominal change in period implies a secular period derivative $\dot{P} = 6.5(5) \times 10^{-11}$ s s^{-1}.

3. DISCUSSION

Here we report *Chandra* observations of the X-ray counterpart of SGR 0526−66. We have three primary results from these observations: (1) We have determined an accurate position for RX J052600.3−660433 (Table 1). (2) We can rule out the pure blackbody (BB) model for the X-ray spectrum. Instead, we find that the best-fit model requires both a BB component and a power-law (PL) component; the photon index, $\Gamma \sim 3.1$, is steep (Table 2). (3) Restricting the period search to a range of 8 s (and its harmonic), we detect periodicity with $P \sim 8$ s in both data sets. If we assume that the period evolves secularly, then $\dot{P} \sim 6.5 \times 10^{-11}$ s s^{-1}. We now discuss these points in more detail.

The accurate position[10] in conjunction with *Hubble Space Telescope* (*HST*) images enabled us to place the most stringent limits to the optical emission from RX J052600.3−660433 (Kaplan et al. 2001). These are the best limits to quiescent optical/IR emission from an SGR. In particular, in Kaplan et al. (2001) we investigated F_{XR}, the ratio of the integrated flux in the X-ray band (i.e., νf_ν) to that in the optical R band. As noted by Hulleman, van Kerkwijk, & Kulkarni (2000), AXPs are distinguished by an unusually large $F_{XR} \sim 10^4$. RX J052600.3−660433 possesses a similarly large F_{XR} (Kaplan et al. 2001)—further evidence of commonality between SGR 0526−66 and the AXPs.

Next, we draw attention to the fact that Γ of RX J052600.3−660433 is decidedly steeper than the value of ~2 found for the quiescent emission from other SGRs (Hurley 2000; Kouveliotou et al. 2001; Fox et al. 2001) but is similar to the values of 3–4 for AXPs (Mereghetti 2001). We view this similarity with considerable interest since AXPs are unique among neutron stars for their steep spectra. Furthermore, we note that a significant fraction of luminosity for both SGRs and AXPs comes out in the X-ray band. Thus, any commonality in the X-ray spectrum takes on additional importance. Indeed, spectral dissimilarity is the reason why the 7.7 s X-ray pulsar 4U 1626−67 is not considered to be an AXP: even though this source shares many attributes with AXPs, it has a flat X-ray spectrum (Angelini et al. 1995).

The possible detection of periodicity in the quiescent emission with $P \sim 8$, similar to the value of the period in the afterglow of 1979 March 5 (Mazets et al. 1979; Cline et al. 1980), is in accord with what has been seen in other SGRs. In particular, a period of about 5 s was detected in the afterglow of the giant flare of 1998 August 27 from SGR 1900+14 (Feroci et al. 2001), and a similar period was also noted in the quiescent emission (Hurley et al. 1999). Returning to RX J052600.3−660433, if we accept that the $\dot{P}$ (based on only two epochs) represents the secular period derivative, then the characteristic age $P/2\dot{P} \sim 2000$ yr and the inferred vacuum dipole field strength, $B^2 = 10^{39} P\dot{P}$, is $B \sim 7 \times 10^{14}$ G. The age is comparable to the estimated age of the SNR N49, ~5000 yr (Vancura et al. 1992), and the inferred B values are similar to those inferred for other magnetars and AXPs (Kouveliotou et al. 1998; Mereghetti 2001).

[10] The position reported here has been corrected using the latest aspect solutions and has higher precision than that given in Kaplan et al. (2001).

4. RAMIFICATIONS AND SPECULATIONS

In the previous section, we summarized our principal observational results: the broadband spectrum and evidence for periodicity in RX J052600.3−660433, the X-ray counterpart of SGR 0526−66. Here we consider the ramifications of the broadband X-ray spectrum, specifically the steep value of the photon index of the power-law component, $\Gamma \sim 3.1$, intermediate to the $\Gamma \sim 2$ of SGRs and $\Gamma \sim 3$–4 of AXPs. There are two interesting consequences of this finding.

First, the intermediate value of Γ is suggestive of SGR 0526−66 providing an evolutionary link between SGRs and AXPs. For both SGRs and AXPs, the PL component has more energy than the BB component; this is especially true of RX J052600.3−660433 and AXPs (see below). This and the continuity in Γ lead us to propose that the PL component is a manifestation of the underlying physical parameter that determines whether a magnetar is an SGR or an AXP. Along these lines, we note that Kaspi et al. (2001) find that the timing noise of AXP 1E 1048.1−5937 is considerably worse than those of other AXPs. Curiously enough, of all the AXPs, this object has the smallest PL index, $\Gamma \sim 2.5$, and has recently been seen to emit small bursts (Gavriil et al. 2002). Thus, both SGR 0526−66 and 1E 1048.1−5937 appear to be "transition" objects between the two classes. Furthermore, Marsden & White (2001) find a correlation between spectral hardness (essentially the PL index) and $\dot{P}$ (which usually correlates with timing noise; Arzoumanian et al. 1994; Gavriil & Kaspi 2002). Thus, from these entirely independent considerations, once again there is a suggestion of Γ being a parameter that varies smoothly from AXPs to SGRs.

Second, the steep value argues that the power law (PL) component dominates the energy output. Specifically, as can be seen from Table 2, the PL flux, even when restricted to photons above 0.5 keV, dominates over the blackbody. We do not know at what (low) energy the PL component cuts off. It is clear from the faint optical flux of RX J052600.3−660433 (Kaplan et al. 2001) that the PL component must turn over somewhere between 0.5 keV (the lowest channel in which we have some detection) and the optical, and the location of this turnover determines the luminosity of RX J052600.3−660433. For instance, if the PL component turns over at 50 eV, then the PL flux will be 150 times larger than the BB flux. The best way (or the only way, to our knowledge) to constrain the low-energy cutoff is by calorimetry via nebular recombination lines.

Above we have argued that the PL component is a manifestation of the underlying physical parameter that determines whether a magnetar is an AXP or SGR. What physical parameter determines Γ? One possibility is the geometry of the magnetic field. AXPs have smooth dipole fields, and SGRs have tangled (multipolar) fields. The latter may then suffer from frequent magnetic reconnections and thus account for the superflares. The pulse fractions (defined as in § 2.3) appear to favor this simple idea: AXPs have large pulse fractions (Özel, Psaltis, & Kaspi 2001), between 30% and 70% (with the exception of 4U 0142+61, for which the pulse fraction is 10%), whereas SGRs have small fractions, 10%–20% for the quiescent counterparts of SGR 0526−66 (this work), SGR 1900+14 (Hurley et al. 1999), and SGR 1806−20 (Kaplan et al. 2002). One expects multipole fields to decay more rapidly compared to dipole fields, and thus in this framework, SGRs should be younger than AXPs. However, the current data, namely, the association of three AXPs with SNRs, taken at face value, seemingly argue for the opposite conclusion. We do recognize that this inference is based on a small sample: six AXPs, three of which have associated SNRs, and at most one SNR association for SGRs (namely, the object of this paper).

Differing geometry can also be due to large-scale twists of a dipole field with the twist angle being the underlying physical parameter (Thompson, Lyutikov, & Kulkarni 2002). In this model, the BB flux arises both from the heating of the surface due to the decay of strong magnetar fields (Thompson & Duncan 1996; Heyl & Kulkarni 1998) as well as heating of the surface by the return current. Resonant cyclotron scattering of these photons by the magnetosphere is responsible for the PL component. The twist angle could be the underlying physical parameter that differentiates AXPs from SGRs. We refer to Thompson et al. (2002) for further discussion of this hypothesis.

As noted in § 1 and also above, there are considerable difficulties in linking AXPs to SGRs via temporal evolution. Specifically, the period and period derivatives of AXPs and SGRs overlap and are strongly clustered. Thus, the simplest interpretation of the overlap of properties is that AXPs and SGRs are similar objects but in differing "states." As an example, we note that SGR 0526−66 behaved like a classical SGR from its discovery in 1979 until 1983 but has been silent since then, and this may account for why the current spectral properties of SGR 0526−66 are similar to those of AXPs.

We do not know the duty cycle of the two states (AXP and SGR). If magnetars spend a significant fraction of time in the AXP state, then the radiated energy (assuming, say, 50 eV low-energy cutoff for the PL component) can be as high as 1.2×10^{37} ergs $s^{-1} \times 10^4$ yr $\sim 3 \times 10^{48}$ ergs. The inferred B-field value (to supply this energy) is in excess of 10^{15} G. As noted in § 1, there is growing evidence for pulsars with strong B fields, 10^{13} G $\lesssim B \lesssim 10^{14}$ G (HBPSRs). Zhang & Harding (2000) have suggested that neutron stars with $B \gtrsim 10^{14}$ G will not exhibit radio pulsations. If so, there may exist an intermediate group of neutron stars with 10^{14} G $\lesssim B \lesssim 10^{15}$ G that are neither radio pulsars nor members of the AXP + SGR family. Perhaps the nearby X-ray pulsar RBS 1223 (Hambaryan et al. 2002) may be a member of this intermediate group.

We have made extensive use of the SIMBAD database, and we are grateful to the astronomers at the Centre de Données Astronomiques de Strasbourg for maintaining this database. We thank Marten van Kerkwijk, Chris Thompson, Andrew Melatos, and Bing Zhang for helpful discussions. D. L. K. thanks the Fannie and John Hertz Foundation for a fellowship. Support for this work was provided by the National Aeronautics and Space Administration through Chandra award GO1-2056X issued by the *Chandra X-Ray Observatory* Center, which is operated by the Smithsonian Astrophysical Observatory for and on behalf of NASA under contract NAS8-39073.

REFERENCES

Angelini, L., White, N. E., Nagase, F., Kallman, T. R., Yoshida, A., Takeshima, T., Becker, C., & Paerels, F. 1995, ApJ, 449, L41
Arzoumanian, Z., Nice, D. J., Taylor, J. H., & Thorsett, S. E. 1994, ApJ, 422, 671
Balucinska-Church, M., & McCammon, D. 1992, ApJ, 400, 699
Bevington, P. R., & Robinson, D. K. 1992, Data Reduction and Error Analysis for the Physical Sciences (2d ed.; New York: McGraw-Hill)
Camilo, F., Kaspi, V. M., Lyne, A. G., Manchester, R. N., Bell, J. F., D'Amico, N., McKay, N. P. F., & Crawford, F. 2000, ApJ, 541, 367
Cline, T. L., et al. 1980, ApJ, 237, L1
de Jager, O. C., Raubenheimer, B. C., & Swanepoel, J. W. H. 1989, A&A, 221, 180
Duncan, R. C., & Thompson, C. 1992, ApJ, 392, L9
Evans, W. D., et al. 1980, ApJ, 237, L7
Feroci, M., Hurley, K., Duncan, R. C., & Thompson, C. 2001, ApJ, 549, 1021
Fox, D. W., Kaplan, D. L., Kulkarni, S. R., & Frail, D. A. 2001, ApJ, submitted (astro-ph/0107520)
Gaensler, B. M., Slane, P. O., Gotthelf, E. V., & Vasisht, G. 2001, ApJ, 559, 963
Gavriil, F. P., & Kaspi, V. M. 2002, ApJ, 567, 1067
Gavriil, P., Kaspi, V. M., & Woods, P. M. 2002, Nature, 419, 142
Hambaryan, V., Hasinger, G., Schwope, A. D., & Schulz, N. S. 2002, A&A, 381, 98
Heyl, J. S., & Kulkarni, S. R. 1998, ApJ, 506, L61
Hulleman, F., van Kerkwijk, M. H., & Kulkarni, S. R. 2000, Nature, 408, 689
Hurley, K. 2000, in Gamma-Ray Bursts: 5th Huntsville Symp., ed. R. M. Kippen, R. S. Mallozi, & G. J. Fishman (Melville: AIP), 763
Hurley, K., et al. 1999, ApJ, 510, L111
Kaplan, D. L., Fox, D. W., Kulkarni, S. R., Gotthelf, E. V., Vasisht, G., & Frail, D. A. 2002, ApJ, 564, 935
Kaplan, D. L., Kulkarni, S. R., van Kerkwijk, M. H., Rothschild, R. E., Lingenfelter, R. L., Marsden, D., Danner, R., & Murakami, T. 2001, ApJ, 556, 399
Kaspi, V. M., & Gavriil, F. P. 2002, IAU Circ., 7924, 3
Kaspi, V. M., Gavriil, F. P., Chakrabarty, D., Lackey, J. R., & Muno, M. P. 2001, ApJ, 558, 253
Kouveliotou, C., et al. 1998, Nature, 393, 235
———. 2001, ApJ, 558, L47
Marsden, D., Rothschild, R. E., Lingenfelter, R. E., & Puetter, R. C. 1996, ApJ, 470, 513
Marsden, D., & White, N. E. 2001, ApJ, 551, L155
Mazets, E. P., Golentskii, S. V., Ilinskii, V. N., Aptekar, R. L., & Guryan, I. A. 1979, Nature, 282, 587
Mereghetti, S. 2001, in The Neutron Star–Black Hole Connection, ed. C. Kouveliotou et al. (NATO ASI Ser. C, 567; Dordrecht: Kluwer), 369
Mereghetti, S., & Stella, L. 1995, ApJ, 442, L17
Özel, F., Psaltis, D., & Kaspi, V. M. 2001, ApJ, 563, 255
Paczyński, B. 1992, Acta Astron., 42, 145
Pivovaroff, M. J., Kaspi, V. M., & Camilo, F. 2000, ApJ, 535, 379
Rothschild, R. E., Kulkarni, S. R., & Lingenfelter, R. E. 1994, Nature, 368, 432
Thompson, C., & Duncan, R. C. 1993, ApJ, 408, 194
———. 1996, ApJ, 473, 322
Thompson, C., Lyutikov, M., & Kulkarni, S. R. 2002, ApJ, 574, 332
Vancura, O., Blair, W. P., Long, K. S., & Raymond, J. C. 1992, ApJ, 394, 158
van Paradijs, J., Taam, R. E., & van den Heuvel, E. P. J. 1995, A&A, 299, L41
Weisskopf, M. C., Tananbaum, H. D., Van Speybroeck, L. P., & O'Dell, S. L. 2000, Proc. SPIE, 4012, 2
Zhang, B., & Harding, A. K. 2000, ApJ, 535, L51